Silicon Chemistry

International Edition: DOI: 10.1002/anie.201510477
German Edition: DOI: 10.1002/ange.201510477

A Disilene Base Adduct with a Dative Si–Si Single Bond

Julia I. Schweizer, Markus G. Scheibel, Martin Diefenbach, Felix Neumeyer, Christian Würtele, Natalia Kulminskaya, Rasmus Linser, Norbert Auner, Sven Schneider, and Max C. Holthausen**

Dedicated to Professor Herbert Roesky on the occasion of his 80th birthday

Abstract: *An experimental and theoretical study of the base-stabilized disilene* ***1*** *is reported, which forms at low temperatures in the disproportionation reaction of* Si_2Cl_6 *or neo-*Si_5Cl_{12} *with equimolar amounts of* NMe_2Et*. Single-crystal X-ray diffraction and quantum-chemical bonding analysis disclose an unprecedented structure in silicon chemistry featuring a dative Si→Si single bond between two silylene moieties,* $Me_2EtN{\rightarrow}SiCl_2{\rightarrow}Si(SiCl_3)_2$*. The central ambiphilic* $SiCl_2$ *group is linked by dative bonds to the amine donor and the bis(trichlorosilyl)silylene acceptor, which leads to push–pull stabilization. Based on experimental and theoretical examinations a formation mechanism is presented that involves an autocatalytic reaction of the intermediately formed anion* $Si(SiCl_3)_3^-$ *with neo-*Si_5Cl_{12} *to yield* ***1****.*

Ever since the seminal work of West et al.,[1] substantial research efforts have been devoted to the preparation of isolable silylenes and disilenes stabilized by intramolecular electronic effects and/or steric protection.[2] More recently the strongly stabilizing properties of *N*-heterocyclic carbene (NHC) ligands[3] have most successfully been exploited to intercept and characterize an impressive variety of compounds with silicon in unusual oxidation states or coordination environments.[4] Remarkable examples include transient species such as SiX_2 (X = Cl, Br, I).[5] Coordination of the strongly σ-donating NHC ligands suppresses the high electrophilicity of the ambiphilic dihalosilylenes. The resulting adducts exhibit an enhanced nucleophilic character that enables further donor–acceptor chemistry with Lewis acidic partners (LA). Such adducts have been identified as interesting synthetic building blocks,[4a,6] exemplified by the crystallographically characterized series NHC→$SiCl_2$→LA.[6,7]

[*] J. I. Schweizer, Dr. M. Diefenbach, F. Neumeyer, Prof. Dr. N. Auner, Prof. Dr. M. C. Holthausen
Institut für Anorganische Chemie, Goethe-Universität
Max-von-Laue-Straße 7, 60438 Frankfurt/Main (Germany)
E-mail: Max.Holthausen@chemie.uni-frankfurt.de
Dr. M. G. Scheibel, Dr. C. Würtele, Prof. Dr. S. Schneider
Institut für Anorganische Chemie, Georg-August-Universität
Tammannstraße 4, 37077 Göttingen (Germany)
E-mail: Sven.Schneider@chemie.uni-goettingen.de
Dr. N. Kulminskaya, Dr. R. Linser
Department NMR-Based Structural Biology
Max-Planck Institute for Biophysical Chemistry
Am Fassberg 11, 37077 Göttingen (Germany)
Supporting information and ORCID(s) from the author(s) for this article are available on the WWW under http://dx.doi.org/10.1002/anie.201510477.

The role of dichlorosilylene as key intermediate in base-induced disproportionation reactions of Si_2Cl_6 has long been postulated,[8] but evidence was only recently provided upon trapping of an $SiCl_2$·NHC adduct[9] and in situ NMR detection of an $SiCl_2$·NMe_2Et adduct in the course of the amine-induced formation of *neo*-Si_5Cl_{12}.[10] The latter reaction represents one of the few preparatively simple routes for the selective synthesis of higher perchlorosilanes.[8,11] Aiming at more comprehensive mechanistic insight we revisited the amine-induced disproportionation of Si_2Cl_6 to identify further reactive key species. Herein, we report the synthesis and characterization of compound **1** (Scheme 1) in high isolated

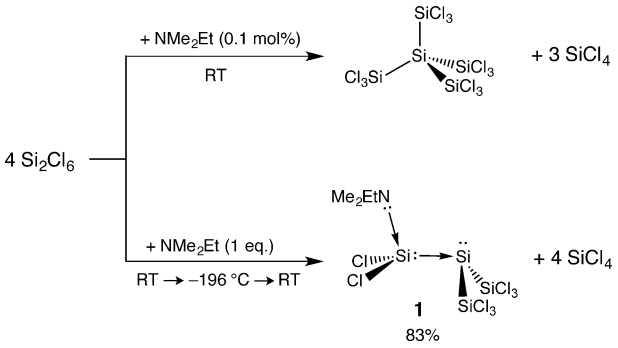

Scheme 1. Preparation of *neo*-Si_5Cl_{12} and **1** from Si_2Cl_6 and NMe_2Et.

yields, which represents a base-stabilized perchlorodisilene. The strongly bent structural motif, unprecedented in silicon chemistry, arises from distinctively different donor–acceptor properties of two silylene building blocks, which are linked by a dative Si→Si single bond. A mechanistic scenario for the selective formation of **1** is presented that is in line with all experimental observations.

In contrast to the use of catalytic amounts of NMe_2Et, *neo*-Si_5Cl_{12} was not observed upon reaction of Si_2Cl_6 with equimolar amounts of the amine. Instead, monitoring the reaction in [D_8]toluene at −50 °C by $^{29}Si\{^1H\}$ NMR spectroscopy reveals exclusively three previously unobserved resonances at 43.7, 27.9, and −155.6 ppm besides $SiCl_4$ (−18.5 ppm). Warming to room temperature results in rapid decay, accompanied by the formation of a red oil that escaped identification so far. However, quick freeze-quench of the reaction in benzene enables the isolation of the transient intermediate **1** as colorless, analytically pure crystals. This compound is stable in the solid state at −30 °C over several weeks, while decomposition in benzene or toluene at ambient

temperatures also gives a red oil. ^{29}Si CP/MAS NMR spectroscopy of isolated **1** fully reproduces the solution NMR spectrum. Furthermore, CP buildup experiments confirmed the absence of directly bonded protons for all Si sites. Solution ^{1}H–^{29}Si HMBC NMR spectroscopy of an isolated sample demonstrates the presence of an amine ligand bound to the silicon site resonating at δ ^{29}Si = 43.7 ppm.

Single-crystal X-ray diffraction analysis revealed the molecular structure of compound **1** (Figure 1), which is in full agreement with all spectroscopic characteristics. The structure features Si1 and Si2 in unusual coordination environments, in analogy to the recently reported germanium compound (NHC)$GeCl_2Ge(GeCl_3)_2$.[12] The coordination polyhedron about Si2 indicates the presence of a stereochemically active electron lone pair. All three Si–Si bond lengths in this molecule (2.324(2)–2.310(2) Å) are very close to those in *neo*-Si_5Cl_{12} (2.338(3) Å)[10] and even to the longest Si=Si bond reported for a disilene (2.2890(13) Å).[13]

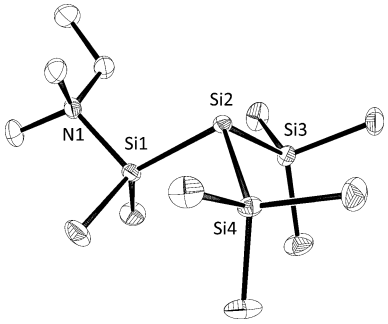

Figure 1. Molecular structure of **1** (thermal ellipsoids displayed at 50% probability level; hydrogen atoms and C_6D_6 solvent molecule not shown). Selected bond lengths [Å] and angles [°]: N1–Si1 1.894(5), Si1–Si2 2.324(2), Si2–Si3 2.310(2), Si2–Si4 2.317(2); N1-Si1-Si2 107.14(15), Si1-Si2-Si3 96.90(8), Si1-Si2-Si4 96.93(8), Si3-Si2-Si4 97.46(8).

Spectroscopic features and bonding were evaluated by density functional theory (DFT) computations.[14] Spin-orbit relativistic ^{29}Si NMR chemical shift calculations[15] on **1** are in good agreement with the observed signatures and confirm the assignment from 2D ^{1}H–^{29}Si NMR spectroscopy (cf. Supporting Information). Natural bond orbital (NBO) analysis reveals a natural localized molecular orbital (NLMO, Figure 2a) that represents an electron lone pair at Si2 with predominant s-character. Two further NLMOs correspond to localized 2e–2c single bonds between N1–Si1 and Si1–Si2, both significantly polarized. Accordingly, natural population analysis (NPA) of **1** indicates a substantial net electron transfer between the respective donor–acceptor fragments (0.24 e for N→Si and 0.69 e for Si→Si; Figure 2b).

Topological analysis of the computed electron density of **1** by means of Bader's quantum theory of atoms in molecules (QTAIM)[16] yields a molecular graph that encloses bond paths for N1–Si1 and Si1–Si2 (Figure 2c). According to the customary bond classification within QTAIM the N1–Si1 bond is characterized as a strongly polar covalent interaction by a marked shift of the bond-critical point (bcp) towards the more electropositive Si1 site, a relatively large electron density ρ_{bcp}, and a positive Laplacian $\nabla^2\rho_{bcp}$.[17] However, in polar bonding situations commonly discussed as dative bonds, the bcp usually resides close to a nodal surface in the Laplacian distribution,[18] so that the sign of $\nabla^2\rho_{bcp}$ alone is inconclusive for a bond classification.

In such cases it is more instructive to consider the one-dimensional $\nabla^2\rho$ profile along the bond path,[17b] which emphasizes valence shell charge concentrations (VSCCs) originating from two overlapping atomic valence shells. The profile along N1–Si1 exhibits a single pronounced VSCC minimum in the vicinity of the electronegative nitrogen atom and a weak shoulder, corresponding to the second VSCC near Si1, both belonging to the N1 atomic basin (Figure 2d). Importantly, similar characteristics are found for the Si1–Si2

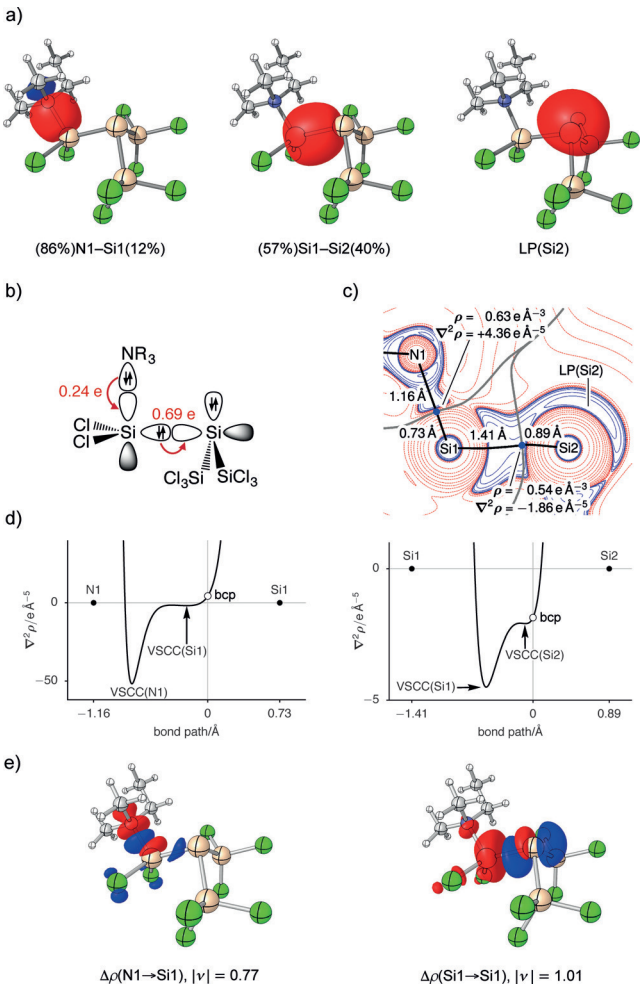

Figure 2. Bonding analysis of **1**. a) NLMOs representing the N1–Si1 and Si1–Si2 bonds and the electron lone pair at Si2. b) Orbital interaction scheme with net electron transfer according to NPA. c) 2D plot of $\nabla^2\rho(\boldsymbol{r})$; charge concentration (blue) and depletion (red), bond paths (black lines), zero-flux surfaces (grey lines), and bcps (blue dots) with characteristic properties and distances to linked atoms. d) 1D Laplacian profiles along the N1–Si1 (left) and Si1–Si2 (right) bond paths. e) Deformation densities $\Delta\rho$ from EDA-NOCV of **1** (charge flow from red to blue): N1→Si1 (left) and Si1→Si2 (right) σ donor interactions. Charge eigenvalues ν quantify the charge transfer between donor and acceptor fragments (in e).

interaction: the bcp is shifted towards Si2 and both VSCC minima reside within the atomic basin of Si1.

Thus both, NBO and QTAIM analyses disclose strong similarities in the nature of the N1–Si1 and the Si1–Si2 bonding interactions. Further characterization of both bonds is possible by energy decomposition analysis with natural orbitals for chemical valency (EDA-NOCV).[19] With reference to neutral closed-shell interacting fragments, which were chosen upon application of the minimum orbital-term energy criterion as advocated by Frenking and co-workers,[20] a single dominant orbital interaction results for either bond (cf. the Supporting Information for a detailed discussion). The resulting deformation densities shown in Figure 2e illustrate the dative nature of these interactions with the direction of charge flow clearly identifying the respective donor and acceptor moieties for both the N1→Si1 and Si1→Si2 bonds. This assignment finds further support by evaluation of Haaland's definition of dative bonds:[21] Heterolytic bond cleavage into NMe_2Et and the disilene $Cl_2Si{=}Si(SiCl_3)_2$ (**2**) is distinctively favored over homolysis into $[NMe_2Et]^{+\cdot}$ and $[\mathbf{2}]^{-\cdot}$ ($\Delta G^{298} = 42$ and 83 kcal mol^{-1}, respectively). Analogously, heterolysis of **1** into $Me_2EtN{\cdot}SiCl_2$ and $Si(SiCl_3)_2$ is favored by far over homolysis into $[Me_2EtN{\cdot}SiCl_2]^{+\cdot}$ and $[Si(SiCl_3)_2]^{-\cdot}$ ($\Delta G^{298} = 36$ vs. 88 kcal mol^{-1}).

We note in passing that **1** represents a molecular manifestation of reactive ("buckled") dimer sites discussed for clean silicon surfaces.[22] Interestingly, while the computed base-free disilene **2** assumes the expected *trans*-bent structure, it retains the almost perpendicular arrangement of the $Si(SiCl_3)_2$ group towards the Si1–Si2 single bond in **1** (bent-angle $\theta = 79.1°$ and $\theta = 78.1°$ in **1** and **2**, respectively).[23] NBO analysis reveals, however, the presence of a σ and a π bond between Si1 and Si2 in **2** (Figure 3). While the σ bond is slightly polarized only, the π bond is strongly polarized towards Si2. Correspondingly, the Wiberg bond index of 1.30 suggests the presence of a partial double bond in **2** (compared to 1.03 for the Si1–Si2 single bond in **1**). This is in tune with the EDA-NOCV results, which disclose two major orbital contributions associated with strongly stabilizing Si1→Si2 σ donation and significantly less efficient Si1←Si2 π backdonation ($\Delta E_1 = -71$ kcal mol^{-1}, $\Delta E_2 = -34$ kcal mol^{-1}, Figure 3).

Turning to the formation mechanism the question arises whether **1** results from Si_2Cl_6 by 1) mere association of the comprising silylenes present as intermediates in the reaction mixture or 2) whether *neo*-Si_5Cl_{12} is initially formed, as with catalytic amounts of amine,[8] followed by immediate decomposition to **1**. In fact, under comparable conditions, *neo*-Si_5Cl_{12} also reacts with equimolar amounts of NMe_2Et in toluene to **1** and $SiCl_4$, which supports hypothesis (2). Furthermore, when conducting this reaction strictly below −70 °C three additional signals ($\delta = 30.9$, −68.8 and −143.1 ppm) were detected by $^{29}Si\{^1H\}$ NMR spectroscopy. Based on the results of spin-orbit relativistic ^{29}Si NMR calculations these signals can be assigned to the $Si^a(Si^bCl_3)_3^-$ anion (Si^a: −137.0 Si^b: 34.2 ppm) and the $(Me_2EtN)_2SiCl_3^+$ cation (calculated for $(Me_3N)_2SiCl_3^+$: −67.7 ppm). Importantly, quantum-chemical evaluation of the formation mechanism of **1** fully supports this assignment (Scheme 2): Initial interaction between NMe_3 as model base and *neo*-Si_5Cl_{12} results in slightly exergonic formation of mono-adduct **A**. From here, the energetically most favored route to $(Me_3N)SiCl_2Si(SiCl_3)_2$ (**1′**) commences with a low-barrier heterolysis of **A** with a second amine to the contact ion-pair

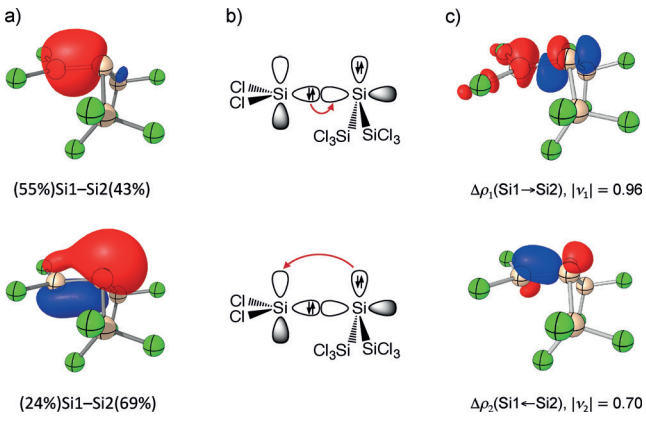

Figure 3. Bonding analysis of **2**. a) NLMOs representing the Si1−Si2 σ (top) and π bonds (bottom). b) Schematic representation of dominant donor–acceptor orbital interactions. c) Deformation densities $\Delta\rho$ from EDA-NOCV of **2** (charge flow from red to blue): Si1→Si2 interaction (top) and Si1←Si2 interaction (bottom). Charge eigenvalues ν quantify the charge transfer between donor and acceptor fragments (in e).

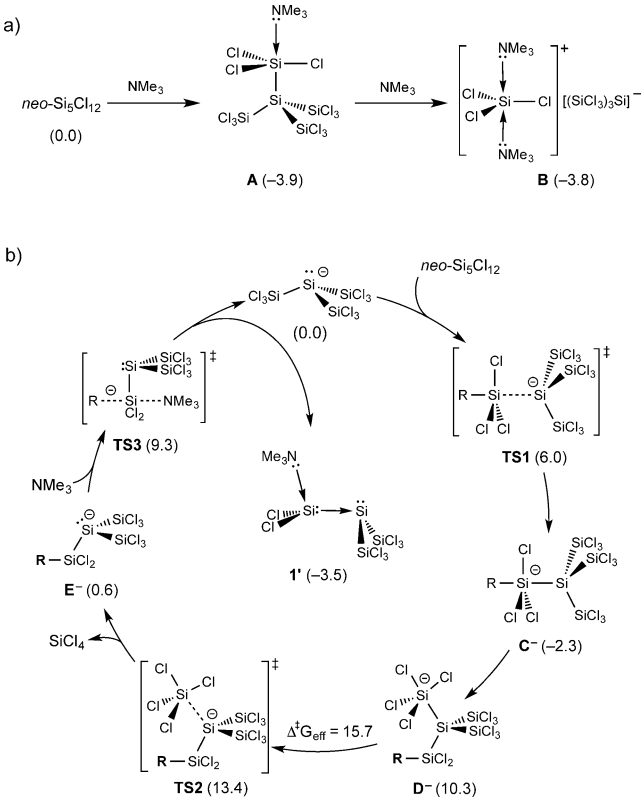

Scheme 2. Computed reaction mechanism. a) Formation of the contact ion-pair **B**. b) Autocatalytic cycle for the formation of **1′**, R = $Si(SiCl_3)_3$ (ΔG^{203} in kcal mol^{-1}; SMD-M06-2X/6-311++G(2d,2p)//6-31+G(d,p); solvent toluene).

$[(Me_3N)_2SiCl_3]^+[Si(SiCl_3)_3]^-$ (**B**) in an overall thermoneutral step. Once formed, the anion $Si(SiCl_3)_3^-$ can add to *neo*-Si_5Cl_{12} yielding silicate $\mathbf{C}^-$ with a minute barrier. After a sequence of low-barrier isomerization steps, akin to related elementary steps identified in earlier work[11b] (see the Supporting Information), thermoneutral elimination of $SiCl_4$ leads to intermediate $\mathbf{E}^-$. This species can undergo an S_N2 type reaction with one equivalent of free amine base to yield **1′** and restore the $Si(SiCl_3)_3^-$ anion. The catalytic cycle computed for the (exergonic) formation of **1′** depicted in Scheme 2b shows an overall effective barrier of 16 kcal mol^{-1}, in agreement with a reaction taking place at −70 °C.

In conclusion, our investigation of the amine-induced disproportionation of Si_2Cl_6 led to the characterization of compound **1**. Based on experimental and computational results, we propose a formation mechanism which emphasizes the role of Si–Si bond heterolysis as opposed to silylene extrusion prevalently assumed for the base-induced disproportionation of perchlorosilanes. Among the resonance structures that appear immediately valid for a phenomenological Lewis representation of **1** (Scheme 3), **1a** is the best

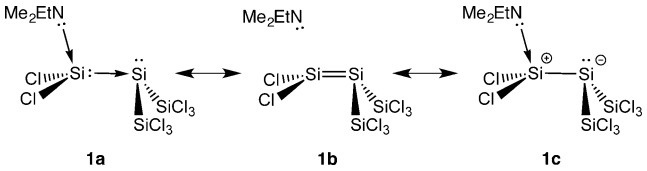

Scheme 3. Plausible Lewis structure representations of **1**.

illustration of our quantum-chemical bonding analysis.[24] It highlights the picture of a central ambiphilic $SiCl_2$ fragment stabilized by push–pull interactions with the amine donor and the $Si(SiCl_3)_2$ moiety serving as LA. To the best of our knowledge **1** thereby features the first structurally characterized dative Si→Si single bond. As such, **1** can be viewed as a base-stabilized $SiCl_2$ tetramer, in line with Rivard's interpretation of his analogous germanium species.[12] At the same time, theory shows that the base-free disilene **2** retains the unusually bent arrangement of the $Si(SiCl_3)_2$ group, so that **1** rightly qualifies as a disilene base-adduct as well (**1b** and **1c** in Scheme 3).[25] The presence of an electron lone pair at Si2 opens ways and means for further donor–acceptor reactivity to higher oligomers. We are currently exploring this hypothesis in our laboratories.

Acknowledgements

J.I.S. gratefully acknowledges a MainCampus scholarship provided by the Stiftung Polytechnische Gesellschaft (Frankfurt). This work was supported by the Beilstein-Institut (Frankfurt) as part of the NanoBiC project eNet and through a Beilstein PhD grant to F.N. Funding is acknowledged by S.S. (DFG INST 186/1086-1) and R.L. (DFG Emmy Noether program, SFB 803, A04; FCI Liebig program). The authors are grateful to Dr. S. Dechert for recording the Raman spectrum of **1**. Computations were performed on the LOEWE-CSC computer cluster.

Keywords: bonding analysis · dative bonds · disilenes · silylenes · X-ray diffraction

How to cite: *Angew. Chem. Int. Ed.* **2016**, *55*, 1782–1786
Angew. Chem. **2016**, *128*, 1814–1818

[1] R. West, M. J. Fink, J. Michl, *Science* **1981**, *214*, 1343–1344.
[2] a) M. Denk, R. Lennon, R. Hayashi, R. West, A. V. Belyakov, H. P. Verne, A. Haaland, M. Wagner, N. Metzler, *J. Am. Chem. Soc.* **1994**, *116*, 2691–2692; b) C. Boehme, G. Frenking, *J. Am. Chem. Soc.* **1996**, *118*, 2039–2046; c) M. Kira, S. Ishida, T. Iwamoto, C. Kabuto, *J. Am. Chem. Soc.* **1999**, *121*, 9722–9723; d) M. Asay, C. Jones, M. Driess, *Chem. Rev.* **2011**, *111*, 354–396; e) B. D. Rekken, T. M. Brown, J. C. Fettinger, H. M. Tuononen, P. P. Power, *J. Am. Chem. Soc.* **2012**, *134*, 6504–6507; f) A. V. Protchenko, K. H. Birjkumar, D. Dange, A. D. Schwarz, D. Vidovic, C. Jones, N. Kaltsoyannis, P. Mountford, S. Aldridge, *J. Am. Chem. Soc.* **2012**, *134*, 6500–6503; g) M. Kira, *Proc. Jpn. Acad. Ser. B* **2012**, *88*, 167–191.
[3] a) M. Soleilhavoup, G. Bertrand, *Acc. Chem. Res.* **2014**, *47*, 256–266; b) M. N. Hopkinson, C. Richter, M. Schedler, F. Glorius, *Nature* **2014**, *510*, 485–496.
[4] a) P. Ghana, M. I. Arz, U. Das, G. Schnakenburg, A. C. Filippou, *Angew. Chem. Int. Ed.* **2015**, *54*, 9980–9985; *Angew. Chem.* **2015**, *127*, 10118–10123; b) M. I. Arz, D. Geiß, M. Straßmann, G. Schnakenburg, A. C. Filippou, *Chem. Sci.* **2015**, *6*, 6515–6524; c) S. U. Ahmad, T. Szilvási, E. Irran, S. Inoue, *J. Am. Chem. Soc.* **2015**, *137*, 5828–5836; d) Y. Wang, M. Chen, Y. Xie, P. Wei, H. F. Schaefer III, P. v. R. Schleyer, G. H. Robinson, *Nat. Chem.* **2015**, *7*, 509–513; e) K. C. Mondal, B. Dittrich, B. Maity, D. Koley, H. W. Roesky, *J. Am. Chem. Soc.* **2014**, *136*, 9568–9571; f) K. C. Mondal, H. W. Roesky, M. C. Schwarzer, G. Frenking, I. Tkach, H. Wolf, D. Kratzert, R. Herbst-Irmer, B. Niepötter, D. Stalke, *Angew. Chem. Int. Ed.* **2013**, *52*, 1801–1805; *Angew. Chem.* **2013**, *125*, 1845–1850; g) M. J. Cowley, V. Huch, H. S. Rzepa, D. Scheschkewitz, *Nat. Chem.* **2013**, *5*, 876–879; h) Y. Xiong, S. Yao, S. Inoue, J. D. Epping, M. Driess, *Angew. Chem. Int. Ed.* **2013**, *52*, 7147–7150; *Angew. Chem.* **2013**, *125*, 7287–7291; i) S. Inoue, C. Eisenhut, *J. Am. Chem. Soc.* **2013**, *135*, 18315–18318; j) K. Leszczyńska, K. Abersfelder, A. Mix, B. Neumann, H.-G. Stammler, M. J. Cowley, P. Jutzi, D. Scheschkewitz, *Angew. Chem. Int. Ed.* **2012**, *51*, 6785–6788; *Angew. Chem.* **2012**, *124*, 6891–6895; k) T. Yamaguchi, A. Sekiguchi, M. Driess, *J. Am. Chem. Soc.* **2010**, *132*, 14061–14063; l) Y. Xiong, S. Yao, R. Müller, M. Kaupp, M. Driess, *Nat. Chem.* **2010**, *2*, 577–580; m) Y. Wang, Y. Xie, P. Wei, R. B. King, H. F. Schaefer III, P. v. R. Schleyer, G. H. Robinson, *Science* **2008**, *321*, 1069–1071.
[5] a) R. S. Ghadwal, H. W. Roesky, S. Merkel, J. Henn, D. Stalke, *Angew. Chem. Int. Ed.* **2009**, *48*, 5683–5686; *Angew. Chem.* **2009**, *121*, 5793–5796; b) A. C. Filippou, O. Chernov, G. Schnakenburg, *Angew. Chem. Int. Ed.* **2009**, *48*, 5687–5690; *Angew. Chem.* **2009**, *121*, 5797–5800; c) A. C. Filippou, Y. N. Lebedev, O. Chernov, M. Straßmann, G. Schnakenburg, *Angew. Chem. Int. Ed.* **2013**, *52*, 6974–6978; *Angew. Chem.* **2013**, *125*, 7112–7116.
[6] R. S. Ghadwal, R. Azhakar, H. W. Roesky, *Acc. Chem. Res.* **2013**, *46*, 444–456.
[7] E. Rivard, *Dalton Trans.* **2014**, *43*, 8577–8586.
[8] G. Urry, *Acc. Chem. Res.* **1970**, *3*, 306–312.
[9] R. S. Ghadwal, K. Pröpper, B. Dittrich, P. G. Jones, H. W. Roesky, *Inorg. Chem.* **2011**, *50*, 358–364.

[10] F. Meyer-Wegner, A. Nadj, M. Bolte, N. Auner, M. Wagner, M. C. Holthausen, H.-W. Lerner, *Chem. Eur. J.* **2011**, *17*, 4715 – 4719.
[11] a) S. B. Choi, B. K. Kim, P. Boudjouk, D. G. Grier, *J. Am. Chem. Soc.* **2001**, *123*, 8117 – 8118; b) J. Tillmann, L. Meyer, J. I. Schweizer, M. Bolte, H.-W. Lerner, M. Wagner, M. C. Holthausen, *Chem. Eur. J.* **2014**, *20*, 9234 – 9239; c) J. Tillmann, J. H. Wender, U. Bahr, M. Bolte, H.-W. Lerner, M. C. Holthausen, M. Wagner, *Angew. Chem. Int. Ed.* **2015**, *54*, 5429 – 5433; *Angew. Chem.* **2015**, *127*, 5519 – 5523; d) J. Tillmann, M. Moxter, M. Bolte, H.-W. Lerner, M. Wagner, *Inorg. Chem.* **2015**, *54*, 9611 – 9618.
[12] S. M. I. Al-Rafia, M. R. Momeni, R. McDonald, M. J. Ferguson, A. Brown, E. Rivard, *Angew. Chem. Int. Ed.* **2013**, *52*, 6390 – 6395; *Angew. Chem.* **2013**, *125*, 6518 – 6523.
[13] T. A. Schmedake, M. Haaf, Y. Apeloig, T. Müller, S. Bukalov, R. West, *J. Am. Chem. Soc.* **1999**, *121*, 9479 – 9480.
[14] Geometry optimizations were performed at the SMD-M06-2X/6-31 + G(d,p) level of theory; improved energies and wave functions were obtained from subsequent SMD-M06-2X/6-311 + + G(2d,2p) single-point calculations. See Supporting Information for full computational details.
[15] C. Zhang, P. Patschinski, D. S. Stephenson, R. Panisch, J. H. Wender, M. C. Holthausen, H. Zipse, *Phys. Chem. Chem. Phys.* **2014**, *16*, 16642 – 16650.
[16] R. F. W. Bader, *Atoms in Molecules: A Quantum Theory*, Oxford University Press, Oxford, **1990**.
[17] a) P. Macchi, A. Sironi in *The Quantum Theory of Atoms in Molecules* (Eds.: C. F. Matta, R. J. Boyd), Wiley-VCH, Weinheim, **2007**; b) P. Macchi, A. Sironi, *Coord. Chem. Rev.* **2003**, *238*, 383 – 412.
[18] a) R. S. Ghadwal, H. W. Roesky, S. Merkel, D. Stalke, *Chem. Eur. J.* **2010**, *16*, 85 – 88; b) P. L. A. Popelier in *The Chemical Bond: Fundamental Aspects of Chemical Bonding* (Eds.: G. Frenking, S. Shaik), Wiley-VCH, Weinheim, **2014**.
[19] M. P. Mitoraj, A. Michalak, T. Ziegler, *J. Chem. Theory Comput.* **2009**, *5*, 962 – 975.
[20] Q. Zhang, W.-L. Li, C.-Q. Xu, M. Chen, M. Zhou, J. Li, D. M. Andrada, G. Frenking, *Angew. Chem. Int. Ed.* **2015**, *54*, 11078 – 11083; *Angew. Chem.* **2015**, *127*, 11230 – 11235.
[21] A. Haaland, *Angew. Chem. Int. Ed. Engl.* **1989**, *28*, 992 – 1007; *Angew. Chem.* **1989**, *101*, 1017 – 1032.
[22] See for example a) G. Mette, M. Reutzel, R. Bartholomäus, S. Laref, R. Tonner, M. Dürr, U. Koert, U. Höfer, *ChemPhysChem* **2014**, *15*, 3725 – 3728; b) M. A. Filler, S. F. Bent, *Prog. Surf. Sci.* **2003**, *73*, 1 – 56, and references therein.
[23] The bent-angle θ is defined as angle between the Si1–Si2 bond and the plane defined by the three silicon atoms of the adjacent silylene fragment; cf. [2g].
[24] For a recent debate on Lewis structure representations of dative bonds in main-group compounds see: a) D. Himmel, I. Krossing, A. Schnepf, *Angew. Chem. Int. Ed.* **2014**, *53*, 370 – 374; *Angew. Chem.* **2014**, *126*, 378 – 382; b) G. Frenking, *Angew. Chem. Int. Ed.* **2014**, *53*, 6040 – 6046; *Angew. Chem.* **2014**, *126*, 6152 – 6158; c) D. Himmel, I. Krossing, A. Schnepf, *Angew. Chem. Int. Ed.* **2014**, *53*, 6047 – 6048; *Angew. Chem.* **2014**, *126*, 6159 – 6160.
[25] For a related disilene fluoride-adduct see: M. Zirngast, M. Flock, J. Baumgartner, C. Marschner, *J. Am. Chem. Soc.* **2008**, *130*, 17460 – 17470.

Received: November 11, 2015
Published online: December 22, 2015

